

Sub-optimal control laws for minimization of take-off distance for aircrafts

Paulo Henriques Iscold Andrade de Oliveira

Ricardo Luiz Utsch de Freitas Pinto

Centro de Estudos Aeronáuticos - Universidade Federal de Minas Gerais.

Copyright © 2006 Society of Automotive Engineers, Inc

ABSTRACT

The present paper presents a method for the numerical determination of control laws for aircrafts needed for optimization of a pre-established maneuver, applied to a take-off under requirements of FAR-Part 23. The methodology is based on the minimization of penalty functions through of mathematical programming algorithms with numerical integration of the aircraft equations of motion. With the optimum control law it is possible to elaborate efficient strategies for automatic flight control and for orientation of piloted flights. Numerical aspects of the application of this procedure are discussed, these being important for their adequate performance. Results are obtained for the optimization of the take-off distance of a tail-wheel airplane and are compared with the take-off distance obtained by manual control.

INTRODUCTION

The present paper presents the application of a methodology for the numerical determination control laws necessary for the optimization of pre-established maneuvers in a sub-optimal form. In particular, the sub-optimal control law for the minimization of the take-off distance for a conventional landing gear aircraft is obtained according to the requirements in the FAR-Part23 regulations. In this problem the objective is to determine the time-history of elevator deflections that minimizes the horizontal distance necessary to allow the take-off and the transposition of an fixed height obstacle. This paper is based on a set of equations of motion proper to symmetric flight, including the non-linearity due to stall effects (Iscold and Pinto, 2004), and includes the landing gear and their interaction with ground.

EQUATIONS OF MOTION

The model of symmetric aircraft motion used in this paper is based on Iscold and Pinto (2004), and includes the traction force provided by the engine group. Figure 1 presents the diagram of forces used for the deduction of the equations of motion.

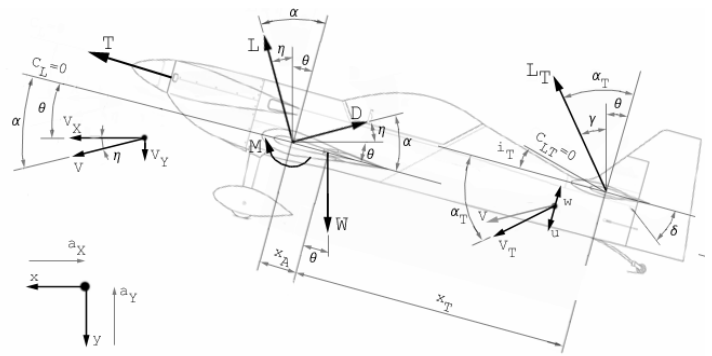


Figure 1 – Forces Diagram

With the state variables defined as:

$$\begin{aligned}
 x_1 &= x \\
 x_2 &= y \\
 x_3 &= \theta \\
 x_4 &= \dot{x} = V_x \\
 x_5 &= \dot{y} = V_y \\
 x_6 &= \dot{\theta} = q
 \end{aligned} \tag{1}$$

the equations of motion can be written as:

$$\begin{cases} \dot{x}_1 = x_4 \\ \dot{x}_2 = x_5 \\ \dot{x}_3 = x_6 \\ \dot{x}_4 = \frac{1}{m} [L \sin \eta - D \cos \eta + L_T \sin \gamma + T \cos x_3 - N_m \mu - N_t \mu] \\ \dot{x}_5 = \frac{1}{m} [-L \cos \eta - D \sin \eta + L_T \cos \gamma - T \sin x_3 + W - N_m - N_t] \\ \dot{x}_6 = \frac{1}{J} [M + L x_A \cos \alpha - L_T x_T \cos \alpha_T + N_m a - N_t b] \end{cases} \quad (2)$$

where:

$$L = \frac{1}{2} \rho(y) S C_L(\alpha) V_R^2$$

$$D = \frac{1}{2} \rho(y) S C_D(\alpha) V_R^2$$

$$M = \frac{1}{2} \rho(y) S \bar{c} C_M(\alpha) V_R^2$$

$$V_R = \sqrt{(x_4 + a_x)^2 + (x_5 + a_y)^2}$$

$$\sin \eta = \frac{(x_5 + a_y)}{V_R}$$

$$\cos \eta = \frac{(x_4 + a_x)}{V_R}$$

$$L_T = \frac{1}{2} \rho(y) S_T C_{LT}(\alpha_T; \delta) V_{RT}^2$$

$$V_{RT} = \sqrt{(x_4 + u_x)^2 + (x_5 + u_y)^2 + \left[\frac{2(x_4 + u_x) \sin x_3}{+2(x_5 + u_y) \sin x_3 + p - w} \right] \cdot (p - w)}$$

$$w \cong \alpha \frac{d\varepsilon}{d\alpha} V_R$$

$$p = x_6 \cdot x_T$$

$$\gamma = \alpha_T - x_3$$

$$\alpha_T = \text{atg} \left(\frac{V_{NT}}{V_{TT}} \right)$$

$$\sin \alpha_T = \frac{V_{NT}}{V_{RT}}$$

$$\cos \alpha_T = \frac{V_{TT}}{V_{RT}}$$

$$V_{TT} = (x_4 + u_x) \cos x_3 - (x_5 + u_y) \sin x_3$$

$$V_{NT} = (x_4 + u_x) \sin x_3 + (x_5 + u_y) \cos x_3 + p - w$$

During the land phase, where is no vertical velocity, the following can be done:

$$x_5 = 0 \quad (3)$$

$$\alpha = \theta = x_3 \quad (4)$$

In (2), N_m and N_t denotes the ground reactions, i.e. the normal force in the main landing gear and in the tail landing gear, respectively, μ denotes the resistance coefficient to roll of the tire-ground group (considering free wheel) and a and b denotes the distances of the main landing gear and the tail landing gear to the aircraft center of gravity, respectively.

The calculation of the normal forces in the landing gear must also receive special attention since it should include the elastic and damping effects. Supposing linearity of these characteristics, the normal forces can be calculated through the following equations:

$$N_m = \begin{cases} \frac{Wb}{a+b} + k_m x_2 & x_2 \leq 0 \\ 0 & x_2 > 0 \end{cases} \quad (5)$$

$$N_t = \begin{cases} \frac{Wa}{a+b} + (x_3 - 15^\circ) k_t + x_6 b_\theta & x_6 \leq 0 \text{ e } x_2 \leq 0 \\ \frac{Wa}{a+b} + (x_3 - 15^\circ) k_t & x_6 > 0 \text{ e } x_2 \leq 0 \\ 0 & x_2 > 0 \end{cases} \quad (6)$$

where k_m denotes the elastic constant of the main landing gear, k_t denotes the elastic constant of the tail landing gear and b_θ denotes the constant of damping of the tail landing gear.

Since what will be analyzed is an aircraft with an internal combustion engine and fixed pitch propeller, it is necessary to provide an available traction curve as a function of the aircraft speed and the percentage of potency which is supplied by the engine. These curves were obtained through the comparison of the potency absorbed by the propeller and the potency available through the engine. With this comparison, it is possible to obtain the rotation in which the propeller will work, given a flight speed and a potency percentage. If this rotation value is known, it is possible to calculate the remaining aerodynamic characteristics of the propeller, such as efficiency and traction force.

Since it regards the analysis of performance of an aircraft in take-off, it is realistic to admit that a maximum potency percentage will be used throughout the entire maneuver. Therefore, the aircraft traction force is a function of the flight speed, exclusively.

TAKE-OFF CONDITIONS ACCORDING TO FAR-PART23

For aircrafts designed according to FAR-Part23, in normal, utility and acrobatic categories, it is required that the

take-off distance be determined including the transposition of a vertical barrier of 50ft (15m). There is also the determination of a speed called *roll speed* which determines the point where the pilot must make some intervention to remove the aircraft from ground. According to this regulation, this speed cannot be lower than the aircraft stall speed. It is also defined that the speed in which the aircraft passes over the obstacle must be superior or equal to 1.2 of the aircraft stall speed.

THE TAKE-OFF PROBLEM: A SIMPLIFIED ANALYSIS

A simplified analysis of the take-off maneuver can be done through a static analysis.

The take-off maneuver by Newton Second Law can be written as (McCormick, 1979):

$$m\ddot{x} = T - D(\theta) - \mu N \quad (7)$$

where T denotes the traction force, D the drag force, and the right-hand last term the rolling resistance force, where μ denotes the rolling resistance coefficient and N the normal force acting on the wheels. This normal force can be written as:

$$N = W - L(\theta) \quad (8)$$

For the land phase it is obvious that the best airplane attitude must maximize the horizontal acceleration, i.e. The pitch angle (θ) must maximize:

$$T - D(\theta) - \mu[W - L(\theta)] \quad (9)$$

For nose-wheel airplanes it is impossible to change the pitch angle during land phase. Then the land-phase optimization depends exclusively of design solutions. But on tail-wheel airplanes is possible to determine an optimal pitch angle time-history during the land phase in order to maximize this function.

On the climb phase, the classic flight mechanics analysis leads to an aerodynamics relation in order to perform a flight with the maximum climb angle. This condition of flight is, obviously, the best flight attitude in order to minimize the horizontal distance necessary to transpose a vertical obstacle. For propellers aircrafts the maximum climb angle, as a first approximation, is obtained when the aircraft is flying at the speed of maximum lift and drag ratio (McCormick, 1979), i.e.:

$$\frac{V(\alpha)}{V_{L/D \max}} = 1 \quad (10)$$

Then, at the land phase the optimal attitude can be obtained by controlling the pitch angle (θ), but in the climb

phase the optimal attitude is defined by the airplane attack angle (α).

THE OPTIMIZATION PROBLEM

The optimization problem consists in finding the control law – in the case of longitudinal aircraft motion, the elevator deflection – which executes a take-off run, according to the FAR-Part-23 regulations, with the smallest horizontal distance.

For this task, the optimization problem will be divided, as in previous analysis, into two phases: i) land phase, until roll velocity and ii) the roll and climb phase until the 50ft obstacle.

In the land phase, the objective function to be maximized is, in fact, the instantaneous horizontal acceleration of the aircraft and the search for optimal elevator deflection can be done at each step of the integrator.

In the rolling and climb phase, until the 50 ft obstacle, the objective function to be maximized should be the aircraft climb angle. However, if this approach is used as objective function, in search of the greatest possible climb angle, there will be a tendency to take the aircraft to flight situations that go beyond stall. Also, it is noted that, according to FAR Part-23 regulations, the speed of flight over the obstacle must not be lower than 1.2 of stall speed, which leads to the belief that the aircraft must, while climbing, at least, maintain its speed. Therefore, in the climb phase, the objective function that was adopted is the difference between the aircraft speed and a pre-established velocity which, within the optimization problem, was also a variable to be optimized (V_2).

Another variable to be optimized is the roll velocity (V_1) of the aircraft which, due to regulations, cannot be lower than stall speed, although there are no restrictions to be higher than this value.

Therefore, the optimization problem can be written as:

Minimize

$$d(V_1, V_2)$$

subject to:

$$\begin{cases} V_1 \geq V_s \\ V_2 \geq 1.2V_s \end{cases} \quad (11)$$

where, for each choice of (V_1, V_2) the following accessory problem of optimal control must be solved:

For $t_i \leq t \leq t_j$, find:

$$\delta(t) = \delta_{otimo} = \text{constant} \quad (12)$$

such that:

$$f(\delta) = \begin{cases} -\dot{x}_4(t_k) & \text{se } x_4 < V_1 \\ (x_4(t_k) - V_2)^2 & \text{se } x_4 \geq V_1 \end{cases} \quad (13)$$

is minimized, where:

$$\begin{aligned} j &= i + \Delta_1 \\ k &= i + \Delta_2 \end{aligned} \quad (14)$$

Δ_1 denotes the time interval in which the elevator deflection is maintained constant and Δ_2 denotes the $f(\delta)$ time interval prediction.

Notice that, in order to evaluate the objective function, the integration must be previously performed until t_k , but, in fact, the elevator deflection δ_{otimo} will be really maintained constant only until $t_j \leq t_k$.

In order to guarantee the constraints imposed by FAR-Part 23, wrote by the inequalities(11), a penalty technique can be used. Then, the objective functions(13) can be re-write as:

$$f = \begin{cases} -\dot{x}_4(t_k) + F & \text{se } x_4 < V_1 \\ (x_4(t_k) - V_2)^2 + F & \text{se } x_4 \geq V_1 \end{cases} \quad (15)$$

where the penalty F is evaluated as:

$$\begin{cases} F = 0 & V_1 > 27\text{m/s e } V_2 > 32\text{m/s} \\ F = (V_1 - 27)^2 & V_1 < 27\text{m/s e } V_2 > 32\text{m/s} \\ F = (V_2 - 32)^2 & V_1 > 27\text{m/s e } V_2 < 32\text{m/s} \\ F = (V_1 - 27)^2 + (V_2 - 32)^2 & V_1 < 27\text{m/s e } V_2 < 32\text{m/s} \end{cases} \quad (16)$$

NUMERIC INTEGRATION PROCEEDURE

For the solution of the state equations for the dynamic model it is necessary to use a numeric integrator of adequate precision. For the results presented in this work, a flight simulator was implemented in Simulink-Matlab which uses a fifth order version of the Runge Kutta Method (Press et al, 1992). This version is more precise than the common fourth-order version and is compatible with an adaptive step procedure. Iscold and Pinto (2004) and Press et alli (1992) presented further details regarding this procedure. A broad scope vision of the block diagram of this simulator is shown in Figure 2.

It can be observed that, the diagram includes: i) the dynamic model; ii) the aerodynamic model; iii) the propulsive model and iv) the atmospheric model.

Notice that, with this implementation, it is possible to construct a flight Simulator for manual piloting. With this simulator, a pilot, using a joystick, is able to control the aircraft (in this case, only in the longitudinal motion) and evaluate the aircraft flight characteristics, as well as trying to repeat, manually, the optimal trajectory obtained through the optimization procedure.

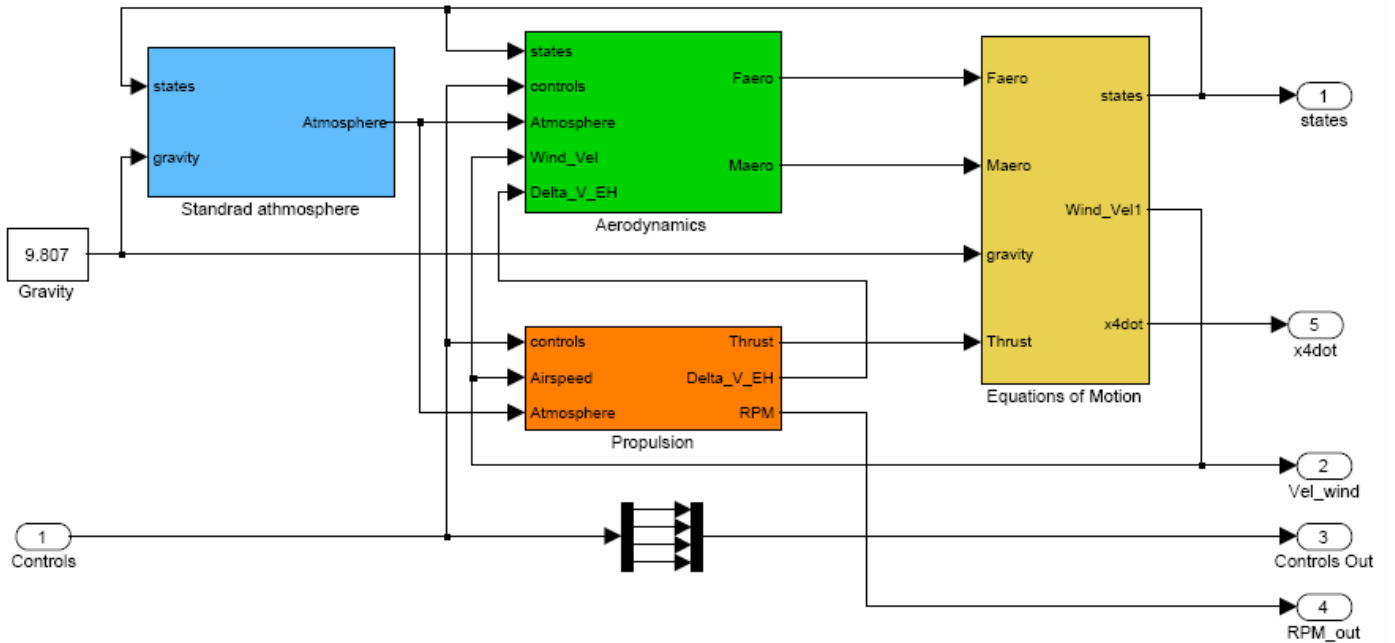


Figure 2 – Dynamic Model

OPTIMIZATION PROCEDURE

A mathematical programming algorithm based on the Nelder-Mead Simplex was used for the optimization procedure. This is a direct search method that does not use gradients.

Basically the method can be explained as follows. If n is the length of x , a simplex in n -dimensional space is characterized by the $n+1$ distinct vectors that are its vertices. At each step of the search, a new point in or near the current simplex is generated. The function value at the new point is compared with the function's values at the vertices of the simplex and, usually, one of the vertices is replaced by the new point, providing a new simplex. This step is repeated until the diameter of the simplex is less than the specified tolerance.

RESULTS

The aircraft CEA-308

For numerical results, the CEA-308 aircraft was used. This aircraft is in development in the Center for Aeronautical Studies of UFMG, with the goal of overcoming the world record in speed in a 3 km circuit for the FAI-C1a0 category of the International Aeronautic Federation.

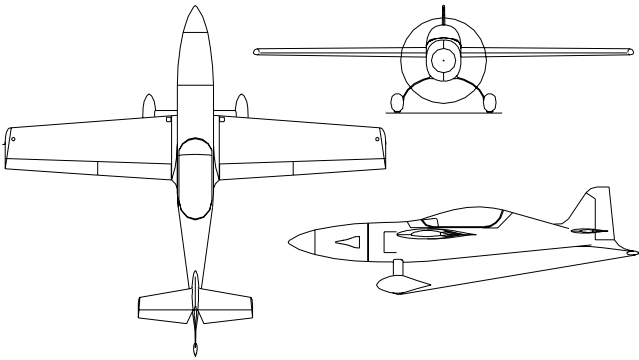


Figure 3 – Three views of the CEA-308 aircraft

The three views of this aircraft are shown in Figure 3. Its main characteristics are presented in Table 1. Its aerodynamic characteristics can be summarized by its drag polar, determined by Iscold (1999) and presented in Figure 4

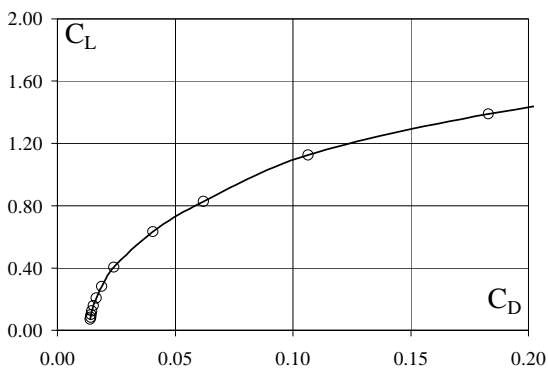


Figure 4 – Drag polar for the CEA-308 aircraft

Table 1 – CEA-308 aircraft characteristics

Number of Seats	1 – monoplace
Span	5.76m
Length	6.36m
Wing area	4.74m ²
Horizontal tail area	1.00m ²
CMA wing	1.1m
Dist. CG – CA HT	3.26m
Dowh-wash	0.4032
Pitch Inertia	33.03kg.m ²
Load Factors	+4.4g/-2.2g
VNE	400 km/h
Empty Weight	190 kgf
MTOW	300 kgf
Power	85 hp

This aircraft is appropriate for this study because: i) it has a conventional landing gear, which increases the relevance of optimization in the land running phase; ii) its take-off distance is handicapped in comparison to its maximum speed, especially due to the fact that it uses fixed pitch propeller.

Optimization Procedure

In order to determine the initial estimation of roll (V_1) and climb speeds (V_2), a search was done in order to obtain take-off distances for different combination of these speeds in the range of 27m/s (stall speed) to 35m/s. The Figure 5 presents the results obtained with this search.

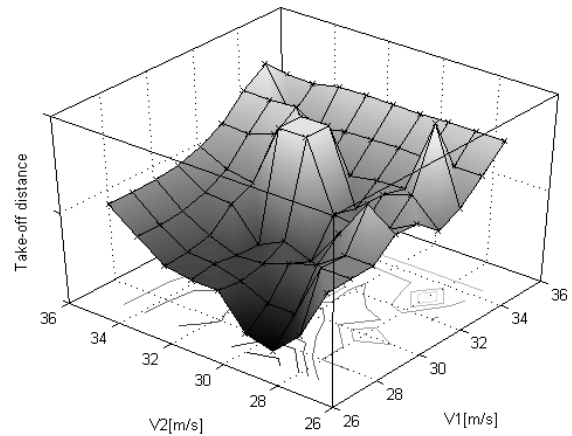


Figure 5 –Take-off distances for different combinations of roll and climb speeds

It is observed that for a roll speed of 27m/s and climb speed of 28m/s, the lowest take-off distance is obtained. However, this climb speed (28m/s) breaks the minimum climb speed constraint imposed by the regulation (32m/s). Thus, a roll speed between 27m/s and 31m/s and climb speed near 32m/s seem to be in the neighborhood of the optimum speeds.

Figure 6 presents the optimum trajectory obtained with the proposed optimization procedure. In this figure, the following are presented: aircraft pitch, horizontal speed,

vertical speed and aircraft height. The values for roll velocity and climb velocity were, respectively, 30.32 m/s and 32m/s. It is observed that the constraint on climb speed (32m/s) is active. The optimum take-off distance was of 410.63m.

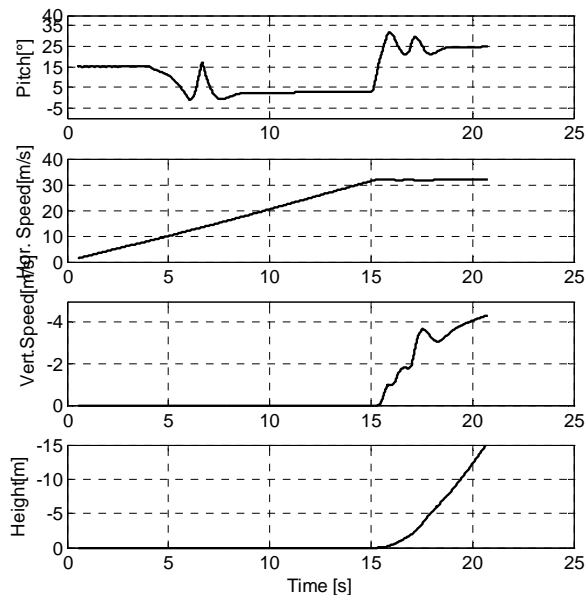


Figure 6 – Optimal Trajectory

Finally, the Figure 7 presents the optimum trajectory obtained through the proposed procedure compared to a trajectory executed manually attempting to follow the optimum roll and climb speeds.

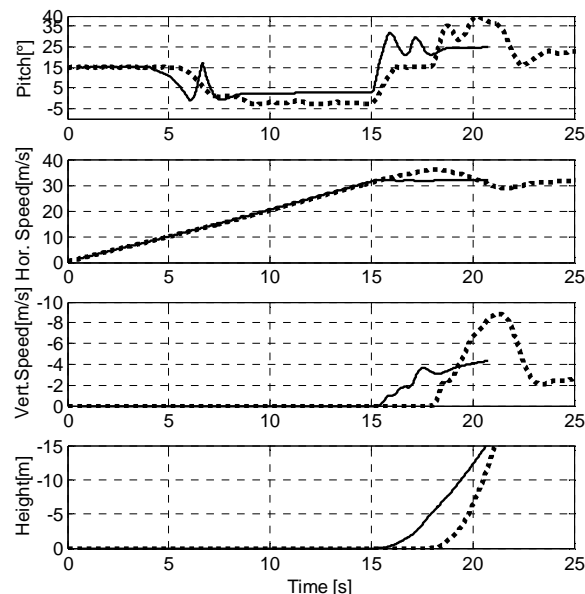


Figure 7 – Optimal trajectory (solid line) compared with manual commanded trajectory (dotted line)

The Figure 8 presents a comparison between both time-histories, the optimum and the manual elevator deflection.

The take-off distance obtained with the manual trajectory (434.12m) is approximately 6% higher than the optimum take-off distance.

These are advantageous values if compared with the usual take-off distance for this aircraft (approximately 600m).

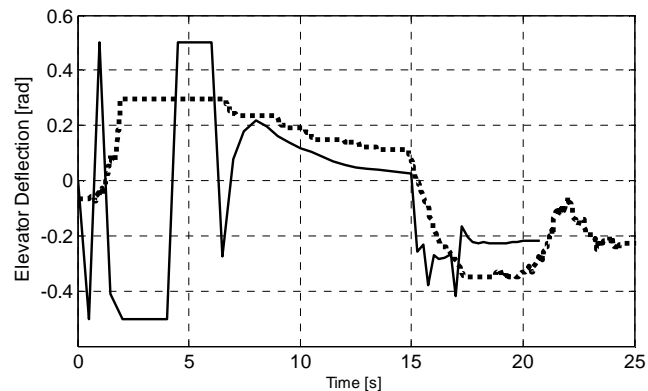


Figure 8 – Comparison between optimal (solid line) and manual (dotted line) elevator deflections

CONCLUSION

A procedure to obtain the optimal elevator time-history to minimize the take-off distance was presented. This procedure take into account the constraints imposed by aviations regulations, specially the vertical obstacle to be transposed and the speed limits. The procedure is based on penalty functions and numerical integrations of the equations of motion.

The optimal results obtained for a practical example were very advantageous and pointed out that it can be used to generate a reference for manual control.

For further studies, the authors pretend include unconsidered aspects such as ground effect and flap deflections.

BIBLIOGRAPHIC REFERENCES

- Etkin, B., 1959, "Dynamics of Flight", John Wiley & Sons, Nova Iorque, EUA.
- Iscold, P. H. A. de O., 1999, "Projeto da Aeronave CEA-308", Centro de Estudos Aeronáuticos da UFMG, Belo Horizonte, Brasil.
- Iscold, P. H. A. de O., 2004, "Um Estudo sobre a Otimização de Trajetórias de Vôo de Planadores de Competição", Relatório de qualificação para defesa de tese de doutorado, UFMG, Belo Horizonte, Brasil.
- Iscold, P., Pinto, R.L.U de F., 2003, "Mathematical modeling for Optimization of Competition Sailplane Flight: A Preliminary Approach", XI Congresso

Internacional da Engenharia da Mobilidade, SAE Brasil, São Paulo, Brasil, 9p.

Luenberger, D. G., 1984, "Linear and Nonlinear Programming", Addison-Wesley Publishing Company, EUA.

McCormick, B. W., 1979, "Aerodynamics, Aeronautics and Flight Mechanics", John, Wiley & Sons, EUA.

Oliveira, P. H. A. de , Pinto, R. L. U. de F., Barros, C. P., 1999, "Um Procedimento Alternativo para Cálculo Aerodinâmico de Aeronaves Leves", Congresso SAE Brasil 1999, São Paulo, Brasil.

Press, W.H., Teukolsky, S.A., Vetterling, W.T., Flannery, B.P., 1992, "Numerical Recipes in FORTRAN 77", Second Edition, Cambridge University Press, Cambridge, USA.